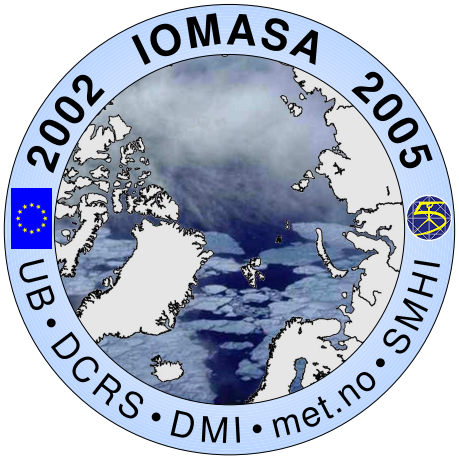

Report for IOMASA Deliverable 1.2.3:

Retrieval algorithm for surface emissivity at AMSU-A frequencies

Nizy Mathew, Christian Melsheimer, Georg Heygster

IUP, University of Bremen

Contents

1 Introduction

The algorithm described in this document retrieves the surface emissivity at window channels of the Advanced Microwave Sounding Unit (AMSU) radiometers in polar regions. The instruments are on the new generation satellites of National Oceanic and Atmospheric administration (NOAA-15, 16, 17). Surface emissivity for all the window channels and for all the scan angles of AMSU is essential for the retrieval of atmospheric parameters with improved accuracy in the lower troposphere using the instrument over polar regions. There are some in-situ measurements [Hewison and English, 1999] and models of surface emissivity [Fuhrhop et al., 1997] but surface emissivity and a method to calculate the emissivity of all different types of polar surfaces, e.g., open water, different types of sea ice, land ice and continent are still required.

2 AMSU Data

The passive microwave radiometer AMSU on the new generation NOAA polar orbiting satellite consists of two modules 'A' and 'B'. The AMSU-A has 15 channels in the frequency range 23 - 89 GHz, with window channels at 23.8, 31.4, 50.3 and 89 GHz. The instrument has an instantaneous field of view (IFOV) of 3.3° at half power points, which provides a spatial resolution of 48 km at nadir. There are 30 measurements on each scan line. The AMSU-B has five channels in the frequency range 89 GHz - 183 GHz with 90 measurements on each scan line. The IFOV of AMSU-B is 1.1° [Goodrum et al., 2000] and the spatial resolution at nadir is about 16 km. The channels at 89 GHz and 150 GHz are window channels. The retrieval of surface emissivity is most accurate for window channels since these measurements are least affected by the atmospheric absorption and emission. The satellite has an orbital inclination of 98°, and the swath width is around 2068 km. This results in the coverage of high latitudes only with the high scan angle portions of the swath. Moreover, the window channels show asymmetric radiance along each scan line [Weng et al., 2003].
The atmospheric contribution to the brightness temperature measurement of the satellite is eliminated by radiative transfer simulations. For the polar regions, in situ measurements from radiosondes are extremely sparse, especially atmospheric profiles over sea ice. The German research vessel Polarstern makes research cruises every year in the polar region. Radiosonde measurements from Polarstern cruises are one possible source of atmospheric profiles [Koenig-Langlo and Marx, 1997]. However, most of the cruises are in summer and it is impossible to get the knowledge of time variation of emissivity from the data. Therefore, we use ECMWF data in a 1.5° grid having 60 vertical levels as the atmospheric profiles. The profiles are available globally, every 6 hours.

3 Method

The total brightness temperature measured by the satellite can be written as

$$\begin{aligned} T_b &= T_u(\nu,\theta) + \varepsilon(\nu,\theta) T_s \mathrm{e}^{-\tau \sec\theta} \\ &\quad + (1-\varepsilon(\nu,\theta)) T_d(\nu,\theta) \mathrm{e}^{-\tau \sec\theta} \end{aligned} \tag{1}$$

where $T_u(\nu,\theta)$ is the up-welling radiation from the atmosphere, T_s is the physical temperature of the surface, ε is the emissivity of the surface, $T_d(\nu,\theta)$ is the down-welling radiation, τ is the to-

tal atmospheric opacity and ν and θ are the observing frequency and incidence angle, respectively. Equation (1) can be solved for the emissivity ε :

$$\varepsilon = \frac{T_b - T_u - T_d e^{-\tau \sec\theta}}{(T_s e^{-\tau(0)\sec\theta} - T_d)e^{-\tau\sec\theta}} \tag{2}$$

Simulating T_b for $\varepsilon = 0$ and $\varepsilon = 1$, (1)) becomes

$$\begin{aligned} T_b(\varepsilon = 0) &= T_u + \varepsilon T_s e^{-\tau\sec\theta} \\ &\quad + (1-\varepsilon)T_d(\nu,\theta)e^{-\tau\sec\theta} \end{aligned} \tag{3}$$

and

$$T_b(\varepsilon = 1) = T_u + T_s e^{-\tau\sec\theta} \tag{4}$$

Substituting (3) and (4) into (2), the equation for emissivity will be obtained as

$$\varepsilon = \frac{T_b - T_b(\varepsilon = 0)}{T_b(\varepsilon = 1) - T_b(\varepsilon = 0)} \tag{5}$$

where T_b is the brightness temperature measured by the satellite for a particular frequency and zenith angle, $T_b(\varepsilon = 0)$ is the simulated brightness temperature with $\varepsilon = 0$ and $T_b(\varepsilon = 1)$ is the simulated brightness temperature with $\varepsilon = 1$. The quantities $T_b(\varepsilon = 0)$ and $T_b(\varepsilon = 1)$ are determined from known atmospheric profiles [Felde and Pickle, 1995].

4 Radiative Transfer Model

The radiative transfer model MWMOD (MicroWave radiative transfer MODel) [Fuhrhop et al., 1997, 1998] is used to simulate $T_b(\varepsilon = 0)$ and $T_b(\varepsilon = 1)$ in (5). MWMOD is designed to compute brightness temperatures for the microwave spectral region, assuming a non-scattering atmosphere and a specular reflecting surface. The model allows the study of the microwave signature of polar regions including the effects of sea ice, ice free ocean and atmosphere. The input to the MWMOD are vertical profiles of temperature, pressure and humidity.

5 Validation

In order to validate the emissivity algorithm, retrieved emissivities over open water were compared with modelled emissivities. The microwave emissivity of open water is well known (provided the wind speed and water temperature are known), here we used the state-of-the-art emissivity model FASTEM (FASt EMissivity). It calculates the permittivity over open ocean based on laboratory measurements of the Debye parameters [English and Hewison, 1998].
The retrieval has been done for all AMSU-A viewing angles and at all four window channels by collocating the radiosonde profiles from Polarstern and AMSU-A overpasses in time interval of ± 3

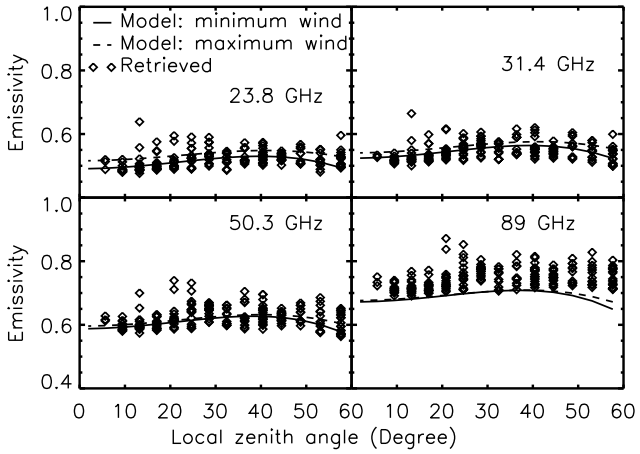

Figure 1: The emissivities retrieved from Polarstern radiosonde profiles and modelled using FASTEM over the Antarctic for all AMSU-A window channels.

hours and space interval of ± 100 km. The maximum and minimum wind speed values and the temperatures from the lowest levels of radiosondes (10m above sea level) are used for modelling. In order to obtain the cloud information, synoptic observations concurrent to the radiosonde launches are used. The results are shown in Fig. 1 (Antarctic) and 2 (Arctic). In both figures, lines represent emissivities modelled by FASTEM and symbols represent the emissivities retrieved. The solid line is for the lowest wind speed and the dashed line for the highest wind speed. Special care has been taken to avoid high emissivity values due to the measurement over the marginal ice zone.

In the Antarctic (Fig. 1), 16 profiles satisfied the conditions of total cloud cover less than 3 octas (3/8) over open ocean. The profiles are from the cruises in the years 2000-2002. The solid lines are for the lowest surface wind of 6.3 ms^{-1} among the profiles and the corresponding surface temperature (271 K). The dashed lines represent the highest surface wind of 16.8 ms^{-1} and the corresponding surface temperature (274.7 K).

In the Arctic there were seven test profiles having less than 3 octas cloud cover. The retrieved emissivity is shown in Fig. 2. Here the emissivities modelled are for surface winds of 2.8 ms^{-1} (solid line) and 28 ms^{-1} (dashed line) and the corresponding temperatures of 278.7 K and 279 K, respectively.

In both the test cases above, the modelling has been done for the two extreme surface winds and the corresponding temperatures in the profiles used. The main factors affecting the ocean surface emissivity are surface wind speed and surface temperature [Wentz, 1983]. Over the Antarctic, because of the particular temperature wind combinations, the modelled emissivities are almost similar and the retrieved emissivities are very close to the modelled ones (Fig. 1). For the lower frequencies, in the Arctic (Fig. 2), the calculated emissivities lie well within the two modelled emissivities. At 89 GHz, the retrieved data seem to have a positive bias. It is the channel that is most sensitive to atmospheric influences, e.g., high water vapour content.

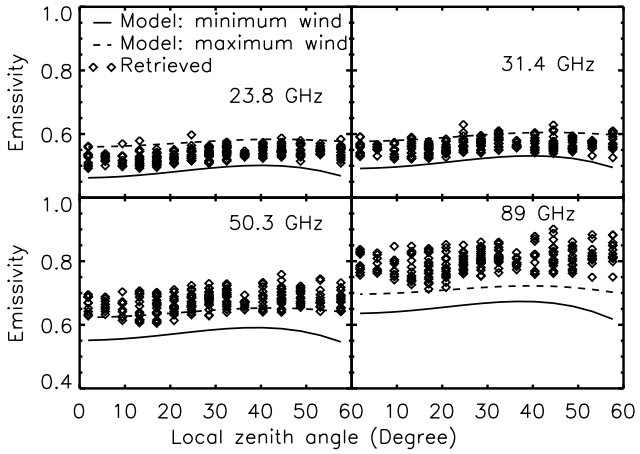

Figure 2: The emissivities retrieved from Polarstern radiosonde profiles and modelled using FASTEM over the Arctic for all AMSU-A window channels

References

S. J. English and T. J. Hewison. A fast generic millimetre-wave emissivity model. *Proceedings of SPIE*, 3503:288–300, 1998.

G. W. Felde and J. D. Pickle. Retrieval of 91 and 150 GHz Earth surface emissivities. *J. Geophys. Res.*, 100(D10):20,855–20,866, October 1995.

R. Fuhrhop, C. Simmer, M. Schrader, G. Heygster, K.-P. Johnson, and P. Schüssel. Study of passive remote sensing of the atmosphere and surface ice. Technical report, Institut für Meereskunde, Kiel, 1997.

R. Fuhrhop, T. C. Grenfell, G. Heygster, K.-P. Johnson, P. S. M. Schrader, and C. Simmer. A combined radiative transfer model for sea ice, open ocean and atmosphere. *Radio Sci.*, 33(2):303–316, March-April 1998.

G. Goodrum, K. B. Kidwell, and W. Winston. *NOAA KLM USER'S GUIDE*. U.S. Department of Commerce, National Oceanic and Atmospheric Administration, 2000.

T. J. Hewison and S. J. English. Airborne retrievals of snow and ice surface emissivity at millimeter wavelengths. *IEEE Trans. Geosci. Rem. Sens.*, 37(4):1871–1879, 1999.

G. Koenig-Langlo and B. Marx. The meteorological information system at the alfred wegener instiute. In M. Lautenschlager and M. Reinke, editors, *Climate and Environmental Database Systems*. Kluwer Academic Publishers, 1997.

F. Weng, L. Zhao, R. R. Ferraro, G. Poe, X. Li, and N. C. Grody. Advanced microwave sounding unit cloud and precipitation algorithms. *Radio Sci.*, 38(4), 2003.

F. J. Wentz. A model function for ocean microwave brightness temperatures. *J. Geophys. Res.*, 88 (C3):1892–1908, February 1983.